ON THE EFFECT OF DIFFERENT MATERIAL CONSTITUTIVE EQUATIONS IN MODELING FRICTION STIR WELDING: A REVIEW AND COMPARATIVE STUDY ON ALUMINUM 6061

M. Nourani, A. S. Milani*, S. Yannacopoulos
School of Engineering, University of British Columbia, Kelowna, Canada

ABSTRACT
In the present article, first a review of various thermomechanical approaches applied to modeling of friction stir welding (FSW) processes is presented and underlying constitutive equations employed by different researchers are discussed within each group of models. This includes Computational Solid Mechanics (CSM)-based, Computational Fluid Dynamics (CFD)-based and Multiphysics (CSM-CFD) models. Next, by employing an integrated multiphysics simulation model, recently developed by the authors for FSW of aluminum 6061, the effect of some common constitutive equations such as power law, Carreau and Perzyna is studied on the prediction of process outputs such as temperature, shear rate, shear strain rate, viscosity and torque under identical welding conditions. In doing so, unknown parameters of the power law dynamic viscosity model were identified for the aluminum 6061 near solidus by fitting the related equation to Perzyna dynamic viscosity model response with the Zener-Hollomon flow stress. Effects of Zener-Hollomon and Johnson-Cook flow stress models are also analyzed in the same example by predicting the shear stress around the FSW tool. Based on the conducted comparative study, some agreeable results and consistencies among outcomes of specific constitutive equations were found, however some clear inconsistencies were also noticed, indicating that constitutive models should be carefully chosen, identified, and employed in FSW simulations based on characteristics of each given process and material.

KEYWORDS: *6061 aluminum alloy, Friction stir welding, Process modeling, Material constitutive equations*

I. INTRODUCTION

Friction stir welding (FSW) is a solid state welding process where a rotating tool consists of a pin and a shoulder is plunged inside the contact surfaces of the welding plates and moved along the weld line [1]. There are different thermomechanical models used to predict physical variables in FSW processes. A major task of these models is the prediction of the material temperature, flow stress, strain rate and strain during processing and the resulting residual stresses after welding. The models solve energy, mass and force equilibrium equations using analytical and numerical approaches such as finite volume, finite difference, and finite element along with different formulations such as Lagrangian/Eulerian /Arbitrary Lagrangian Eulerian (ALE), etc. A key element of any selected FSW prediction model is the fundamental relation used to link the flow stress, temperature, strain, and strain rate, which is commonly referred to as constitutive equation. The form of such equations closely depends on microscopic mechanisms of the plastic flow in crystalline materials, and their constants are obtained based on mechanical experiments such as hot tension, compression or torsion tests [1]. The reported FSW models can be categorized into three main groups as reviewed in Sections 1.1 to 1.3. Within all these categories, heat transfer for temperature predictions is normally an embedded formulation in the models.

1.1 Computational Solid Mechanics (CSM)-based models

These models have been extensively used in earlier research [1-67] and consider that the welding material remains solid during the process. The force equilibrium equation is expressed on the basis of continuum mechanics and the resulting partial derivative equations (PDE) are solved using in-house or commercial codes. The early models in this category have used a thermal model first to predict the temperature distribution in the welded parts and then in a segregated model they could predict the residual stress field [1]. In more recent models under this category, a coupled thermomechanical model is directly used to predict both the temperature distribution and the residual stress fields [65]. Nevertheless, it can be inferred that the main characteristic of the CSM models is the computation of strain and residual stress distributions. Some of the commercial codes used for these models include Abaqus, Ansys, Forge3, and Deform3D.

1.2 Computational Fluid Dynamics (CFD)-based models

Under this category, some models directly use viscosity laws in simulation and some others are based on an equivalent dynamic viscosity definition from CSM models, also called solid mechanics based dynamic viscosity [3, 37, 43, 68-120]. For the latter, the Von-Mises flow stress was first used by Zienkiewicz et al. [121] in modeling viscoplastic deformation processes such as extrusion, rolling, deep drawing and stretching. Using in-house or commercial codes such as Fluent, in these models the momentum equilibrium equation (Navier-Stokes) is solved considering that the non-Newtonian material has different viscosity values equal to the ratio of shear stress to shear strain rate, whose value can vary in different regions of the deformation domain. Hence, the main characteristic of these models is the computation of strain rate, and they are most often not capable of predicting elastic strain and residual stress fields because of the incompressible flow assumption. There are some few cases where a limited plastic strain has been predicted by CFD models using some post-processing techniques such as those by Reynolds et al. [3], Bastier et al. [87], Long et al. [105], and Arora et al. [118]. For instance, Long et al. [105] used a geometry-based formulation to calculate engineering strains on limited streamlines. Reynolds et al. [3], Bastier et al. [87], and Arora et al. [118] estimated the accumulated plastic strains in the welding material by integrating strain rates along limited streamlines.

1.3 Multiphysics (CSM-CFD) models

There are models which use both CFD and CSM approaches to predict strains and residual stresses, along with flow characteristics. Namely, first they use a CFD approach based on the equivalent dynamic viscosity definition from CSM to predict temperature distribution and the shear stress near tool-material interface. Then, they employ the CSM approach to model elastic and plastic strains and residual stresses. The residual stresses are resulted from different thermo-elastic strains across the material domain before and after clamping release in the FSW set-up and complete cooling of plates. These models often use temperature dependent elastic moduli and thermal expansion coefficients [122-126]. If any solid-state phase transformation occurs after FSW with different lattice volume properties of the new phase compared to the parent phase, then transformation induced strains also needs to be considered in residual stress calculations; e.g., in FSW of carbon steels [127, 128]. More details of these models are explained in [129].

Recently, an integrated multiphysics model of FSW of aluminum 6061 was developed in [129] using Comsol. Regarding the ‘integrated’ feature of the model, it is continuously capable of predicting plastic strains and strain rates over the material domain during the process, followed by predicting the microstructure and residual stresses after the process, all within the same code. The strain components at different material points are calculated using the integration of strain rate over time on different flow streamlines. The heat transfer and CFD modules of the model use a viscoplastic material behaviour (fluid type constitutive equation) to find the temperature history. Subsequently it is used as a input in the CSM module with an elasto-viscoplastic constitutive material behaviour (solid type constitutive equation) to find residual stresses resulting from thermo-elastic strains at the end of the welding process after material cools down to ambient temperature and unclamping [126]. It has been shown that using the same model, the weld material microstructure can be predicted by using empirical grain and subgrain size equations [130]. In Kocks-Mecking-Estrin (KME) or Hart’s

constitutive models, the effect of dynamic recrystallization, grain growth and recovery on flow stress has been considered (more to be discussed in Section 2-2), but to the best of authors' knowledge no model has evaluated their effects on the strain softening and the strain distribution during FSW. In the next sections we review different material constitutive equations used most commonly by other researchers within the CSM and CDF model categories (Section 2) and then we implement (Section 3) and compare (Section 4) some of these equations within the same FSW prediction tool developed in [129] for aluminum 6061. Concluding remarks regarding the optimal use of the selected constitutive equations are presented in Section 5, and potential future work is outlined in Section 6.

II. CFD AND CSM CONSTITUTIVE EQUATIONS

There are different constitutive equations defined for different types of welding materials based on the chosen modeling approach (CFD [131] or CSM [132]). Some of these constitutive equations have been previously used in modeling FSW processes, which are discussed below.

2.1 CFD constitutive equations

The important point is that when a CFD approach is used, because it is assumed that the material is an incompressible fluid (based on the mass equilibrium equation), we cannot model elastic deformation. During the deformation of a plastic (or viscoplastic) solid, plastic strains are large enough that one can consider elastic strain to be negligible, then the material behaviour mimics an incompressible viscous flow (possibly non-Newtonian) along with the prescribed velocity boundary conditions. Different formulations for these problems are suggested in [121, 133, 134]. Kuykendall et al. [135] studied the effect of using some of such constitutive equations in stress-strain model of axial compression and compared them with data from experiments. They determined the model constants for Zener-Hollomon, Johnson-Cook and Kockw-Mecking-Estrin constitutive equations for aluminum 5083 and used as input in a model developed for axial compression deformation. Capabilities of the constitutive equations were compared in capturing the strain hardening and saturation in the axial compression model and compared well to experimental stress-strain curves.
There are different fluid-like material behaviors as shown in Figure 1. Generally, these include Newtonian, Bingham plastic, power law (dilatant or pseudoplastic), and structural. The structural fluids have a Newtonian behavior at very high and very low shear rates and have shear thinning or pseudoplastic properties between these two extremes [131].

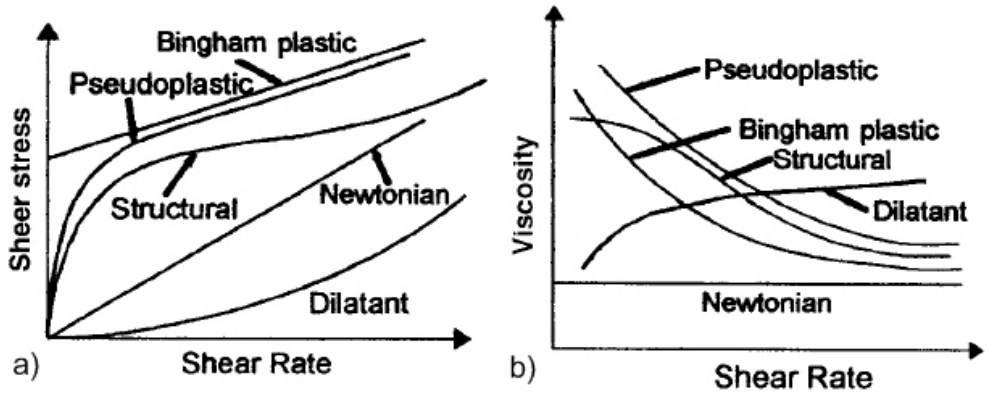

Figure 1: (a) Shear stress versus shear rate and (b) viscosity versus shear rate for different fluid-type materials [131]

General constitutive equations for the fluid-type materials should relate temperature (T), flow stress (σ), and strain rate ($\dot{\bar{\varepsilon}}$) or shear strain rate ($\dot{\gamma}$) to dynamic viscosity (η). It has been shown that the maximum temperature during FSW is solidus temperature, as this welding process is a solid state welding and there is a cut-off temperature (below the solidus temperature) at which the dynamic viscosity of material decreases dramatically. The dynamic viscosity becomes virtually zero when the temperature reaches the solidus temperature [104, 129].

2.1.1 Power law dynamic viscosity

The power law is an example of a generalized non-Newtonian fluid. If there is a linear relation between the logarithm of shear stress and the logarithm of viscosity, then the viscosity of the material under a power-law can be represented as:

Power law dynamic viscosity: $$\eta(\dot{\gamma}) = m\dot{\gamma}^{n-1} \quad (1)$$

where two viscous rheological properties (model constants) are the consistency coefficient *m*, and the flow index *n*,. For $n>1$, the power law represents a shear thickening or pseudoplastic fluid. For $n<1$, it is a shear thinning or dilatant fluid. When the value of *n* is equal to one then it describes a Newtonian fluid. Colegrove et al. [69] and Reynold et al. [3] used the above power-law constitutive model in FSW modeling for the first time. Later, Reynolds et al. [3] presented a temperature dependent power law dynamic viscosity as:

Temperature dependant power law dynamic viscosity: $$\eta(T,\dot{\gamma}) = K\exp(\frac{T_0}{T})\dot{\gamma}^{n-1} \quad (2)$$

2.1.2 Carreau model of dynamic viscosity

The Carreau model [136] has proven to be very effective for describing the viscosity of structural fluids. The constitutive equation under this model reads:

Carreau model [136]: $$\eta(\dot{\gamma}) = \eta_\infty + \frac{\eta_0 - \eta_\infty}{[1+(\lambda^2\dot{\gamma}^2)]^p} \quad (3)$$

where η_0 is the low shear limiting viscosity, η_∞ the high shear limiting viscosity, λ is a time constant, and p is the shear thinning index. Atharifar et al. [117] used the Carreau model in FSW modeling in the following form:

Carreau model [117]: $$\eta = \eta_\infty + (\eta_0 - \eta_\infty)[1+(\dot{\gamma}\lambda\exp(\frac{T_0}{T}))^2]^{\frac{(m-1)}{2}} \quad (4)$$

where η_0 and η_∞ are zero and infinite shear viscosities respectively, $\dot{\gamma}$ is the shear strain-rate, λ is the time constant, T_0 is the reference temperature and *m* is the power law index for the non-Newtonian fluid.

2.1.3 Perzyna model of dynamic viscosity

The dynamic viscosity which is a function of temperature and strain rate can be derived from the ratio of the effective deviatoric flow stress to the effective strain rate by use of Perzyna's model of viscoplasticity [133] as presented by Zienkiewicz et al [134] and employed by Ulysse [70] in FSW modeling:

Perzyna model: $$\eta(T,\bar{\dot{\varepsilon}}) = \frac{\sigma(T,\bar{\dot{\varepsilon}})}{3\bar{\dot{\varepsilon}}} \quad (5)$$

However, in implementing this model one still requires to use a constitutive equation for the effective flow stress, σ, versus effective strain rate, $\bar{\dot{\varepsilon}}$, which in turn is considered one of the equations for CSM approaches as will be discussed in Section 2.2.

2.1.4 Bendzsak-North model of dynamic viscosity

For some aluminum heat-treatable alloys, the Zener-Hollomon (Sellars-Tegart law) used in Perzyna dynamic viscosity equation provides a poor fit to isothermal, isostrain-rate data [71]. In this case it is preferable to interpolate the viscosity property at different temperature and strain rates numerically. An alternative approach has been adopted by Bendzsak et al. [68, 137, 138] who used an effective dynamic viscosity described at a given temperature by a heuristic material model which gives a moderate strain-rate sensitivity to the viscosity.

Bendzsak-North model: $$\eta_a = \eta_0\exp(-B\tau_{r\theta}) \quad , \tau_{r\theta} = 2\eta_a\bar{\dot{\varepsilon}} \quad (6)$$

where η_a is effective viscosity, η_0 is reference viscosity, *B* is material constant, $\tau_{r\theta}$ is shear stress and $\bar{\dot{\varepsilon}}$ is equivalent strain rate. Bendzsak et al. [68] were among first used this constitutive model in FSW modeling.

2.1.5 Modified Bingham model of dynamic viscosity

Perfect yielding material behavior is known as Bingham fluid behavior as shown in Figure 1 and can be implemented by the following constitutive law [109]:

Bingham fluid:
$$\begin{cases} \bar{\tau} < \tau_0 : \bar{\dot{\gamma}} = 0 \\ \bar{\tau} \geq \tau_0 : \bar{\tau} = (\frac{\tau_0}{\dot{\gamma}} + \eta)\bar{\dot{\gamma}} \end{cases} \quad (7)$$

where $\bar{\tau}$ is the equivalent shear stress, τ_0 is the yield shear stress, $\bar{\dot{\gamma}}$ is the equivalent shear strain rate and η is the dynamic viscosity.

Dorfler [109] introduced a modified Bingham equation in FSW modeling by using Papanastasiou approach [139] and also defining a new constant *m* (convergence parameter) to avoid numerical errors during simulations [109]:

Modified Bingham equation:
$$\bar{\tau} = \frac{\sigma(\dot{\gamma}, T)^m}{(\dot{\gamma} + h)^m} . \bar{\dot{\gamma}} \quad (8)$$

The convergence parameter *m* is chosen as exponent in a way that the highly nonlinear term becomes eliminated for $m = 0$ and is fully effective for a value of $m = 1$. The constant *h* is used to achieve convergence when the shear rate is zero and is chosen very small so that it does not affect the accuracy of the model. Dorfler [109] used an empirical flow stress equation which will be explained in Section 2.2 as one of the solid mechanics-based flow stress constitutive equations. He also used a level set method to model material properties in dissimilar FSW. It is worth adding that there are other constitutive equations which have been developed in CFD but have not been used in FSW such as Ellis model, Sisko model, Meter model, Yasuda model [131], and also the formulation of Duvaut–Lions which is equal to the formulation of Perzyna [140].

2.2 CSM constitutive equations

Generally speaking, one can consider different solid mechanics-based material models during plastic deformation of a material. These include perfectly plastic, plastic, elastic-perfectly plastic, elastoplastic, perfectly viscoplastic, viscoplastic, elastic-perfectly viscoplastic and elastoviscoplastic as shown in Figure 2.

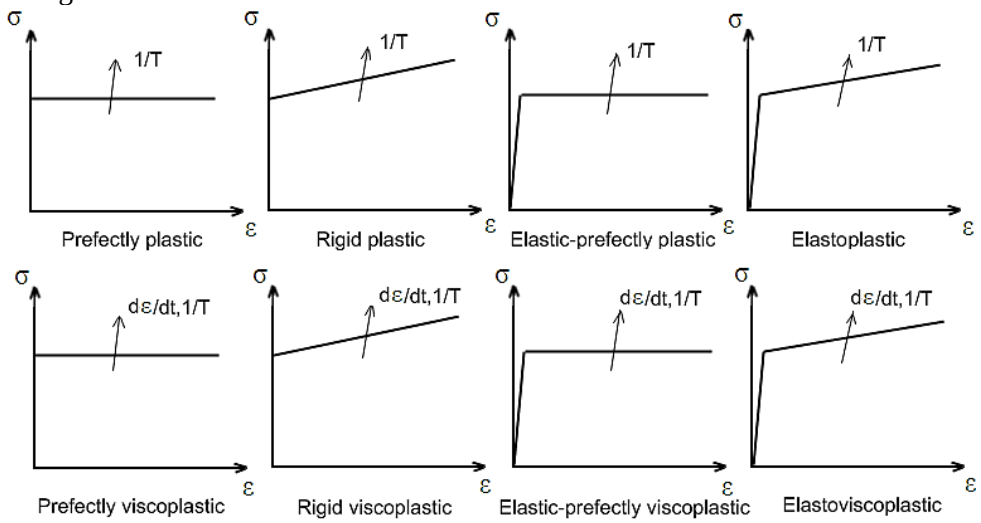

Figure 2: Schematic of stress-strain curves in different solid mechanics-based material models (T is temperature and dε/dt is strain rate)

The material behavior during hot deformation can include dynamic recovery or dynamic recrystallization as shown in Figure 3 [141]. During dynamic recovery, stress reaches the steady state stress (saturation) and during dynamic recrystallization, first the stress increases to the peak stress and then reaches a steady state plateau where there is no change in stress value, but microstructural changes can be present.

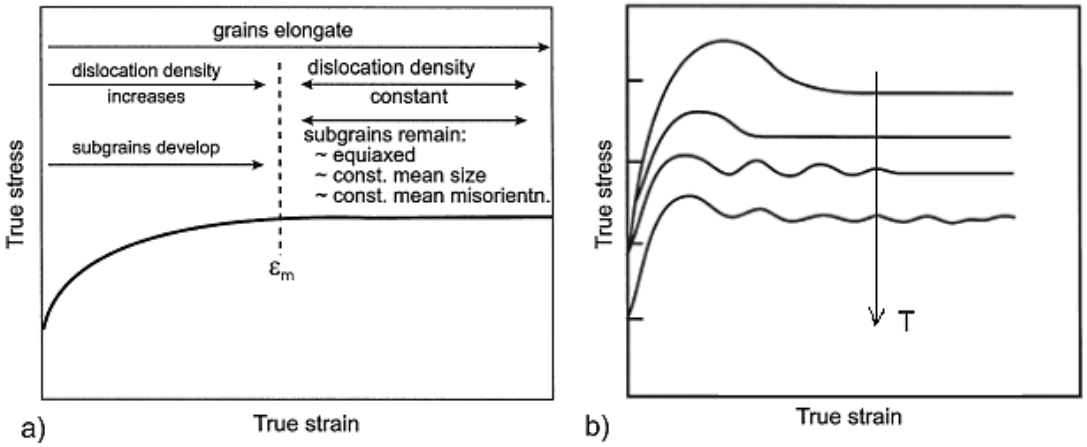

Figure 3: Schematic of the true stress-true strain curve during (a) dynamic recovery, and (b) dynamic recrystallization [141]

In general, CSM-based material constitutive relations in FSW models are aimed to link strain rate ($\dot{\varepsilon}$), temperature (T) and sometimes strain (ε) to the equivalent flow stress (σ). Most commonly used models of this kind are reviewed below.

2.2.1 Zener-Hollomon (ZH) model or Sellars-Tegart law (perfectly viscoplastic)

One may consider the flow stress of a solid during hot deformation to be equal to its dynamic recovery/recrystallization steady state stress which is independent of plastic strain. If the plastic deformation is high, one may also neglect the elastic deformation and consider the material behavior as prefectly viscoplastic as shown in Figure 2. The material flow stress can be correlated with the Zener-Hollomon parameter [142] (temperature-compensated strain rate) as proposed by Sellars and Tegart [143] and modified by Sheppard and Wright [144]:

Zener-Hollomon parameter [143, 144]: $$Z = \dot{\varepsilon} \exp(\frac{Q}{RT}) \quad (9)$$

Zener-Hollomon flow stress model: $$\sigma = \frac{1}{\alpha}\sinh^{-1}((\frac{Z}{A})^{1/n}) \quad (10)$$

where Z is the Zener-Hollomon parameter, $\dot{\varepsilon}$ is the effective strain rate, Q is the temperature independent activation energy which is equal to self-diffusion energy, R is the gas constant, and α, A, and n are model constants which are determined from hot deformation experiments. Tello et al. [145] recently reported more accurate model constants for some alloys compared to available experimental data. This CSM constitutive model has been extensively used in CFD models of FSW, which are essentially based on an equivalent dynamic viscosity definition from a CSM approach by means of Perzyna law [70] (Eq. 5).

2.2.2 Johnson-Cook model (Elastoviscoplastic)

The Johnson-Cook material model is an empirical equation in the following form [146]:

Johnson-Cook model: $$\sigma = [A + B(\bar{\varepsilon}^{pl})^n](1 + C\ln\frac{\dot{\bar{\varepsilon}}^{pl}}{\dot{\varepsilon}_0})[1 - (\frac{T - T_{ref}}{T_{melt} - T_{ref}})^m] \quad (11)$$

where $\bar{\varepsilon}^{pl}$ is the effective plastic strain, $\dot{\bar{\varepsilon}}^{pl}$ is the effective plastic strain rate, $\dot{\varepsilon}_0$ is the normalizing strain rate (typically normalized to a strain rate of 1.0 s^{-1}) and A, B, C, m, n, T_{melt} and T_{ref} are material constants. Askari et al. [5] have been among early researchers who used this constitutive model in FSW, and more recently Grujicic et al. [48, 62, 66] employed a modified version of the Johnson-Cook constitutive equation considering the effect of grain size and dynamic recrystallization on the material flow stress.

2.2.3 Norton-Hoff model (Perfectly viscoplastic)

The Norton-Hoff material is a perfectly viscoplastic material law in which the stress is a power law function of the strain rate as follows.

Norton-Hoff model [148]: $$\sigma = 2K(\sqrt{3}\dot{\bar{\varepsilon}})^{m-1}\dot{\varepsilon} \quad , K = K_0(\varepsilon_0 + \bar{\varepsilon})^n \exp(\frac{\beta}{T}) \quad (12)$$

Where, $\bar{\varepsilon}$ and $\dot{\bar{\varepsilon}}$ are the equivalent strain and the equivalent strain rate, *m* and *n* are the sensitivity indexes to strain rate and strain, respectively, and K_0, ε_0 and β are material constants. If *m* = 1, the material is a Newtonian fluid with viscosity *K*. It is well known that the Norton-Hoff law is an approximation to the Sellars-Tegart law, when the Zener-Hollomon parameter is smaller than *A* (material constant as shown in Eq. 10), i.e., when *Z*<<*A* [147].

The Norton-Hoff law has been widely used in metal forming process simulations, such as hot forging, where the material experiences high strain rate deformations at high temperatures. Fourment et al. [13] have used this constitutive model early in their FSW model, and more recently Assidi et al. [56] used the model with both *K* and *m* being functions of temperature.

2.2.4 Power law model (rigid-viscoplastic)

A temperature and strain rate dependant rigid-viscoplastic material power law model is defined as follows [22]:

Power law model: $$\sigma = KT^{A}(\dot{\bar{\varepsilon}})^{B}(\bar{\varepsilon})^{C} \quad (13)$$

where *K*, *A*, *B* and *C* are material constants calculated by regression of the experimental data. Buffa et al. [22] used this constitutive model in a FSW model in 2006.

The next two constitutive models, as opposed to the previous ones, are microstructurally motivated (with state variables) based on strain hardening of the forming material.

2.2.5 Kocks-Mecking-Estrin (KME) model (rigid-viscoplastic)

This model is valid for pure materials in theory as it considers the effect of storage hardening and dynamic recovery softening mechanisms on dislocation density. It is a classic model in the literature for Al alloys which are strain hardened assuming that the plastic slope ($d\sigma/d\varepsilon$) linearly changes with the flow stress in general situations for instance when precipitates are present. The KME model has the following expression for the flow stress σ_f as a function of the plastic strain ε_p, the dislocation storage rate θ and the recovery rate β: [149-155]:

KME model: $$\frac{d\sigma_f}{d\varepsilon_p} = \theta - \beta(\sigma_f - \sigma_y) \quad (14)$$

σ_y is the material yield strength. The values of θ and β are obtained by a linear fit on the variation of the strain hardening rate $\frac{d\sigma_f}{d\varepsilon}$ with the true flow stress in plasticity (σ_{pl}). Eq. (14) was identified by Voce empirically [152]. Simar et al. [67] used an extended KME constitutive model in FSW modeling, which accounts for dynamic precipitation and Orowan loop during the calculation of θ and β.

2.2.6 Hart's model (rigid viscoplastic)

Dynamic recovery and hardening occur simultaneously during deformation and hence, any flow stress change is the result of both of these mechanisms by means of generation and annihilation of crystal defects such as dislocations. Hart [153] proposed a new constitutive equation which was later used by Eggert and Dawson [154, 155] in modeling of upset welding and by Forrest et al. [21] in FSW modelling. The simplified Hart's model considers the plastic stress (τ^p) and the viscous stress (τ^v) affecting the flow stress (σ) as follows [27, 33, 85]:

Hart's model: $$\sigma = \tau = \tau^p + \tau^v \quad (15)$$

$$\tau^v = G\left(\frac{\bar{D}}{a}\right)^{1/M} \quad , a = a_0 \exp\left(-\frac{Q'}{RT}\right) \quad (16)$$

$$\tau^p = K\exp\left[-\left(\frac{b}{\bar{D}}\right)^{\lambda}\right] \quad , b = b_0\left(\frac{K}{G}\right)^{N}\exp\left(-\frac{Q}{RT}\right) \quad (17)$$

where $\bar{D}$ is the average value of deformation rate, *T* is temperature and *K* is strength. *G*, *Q*, *Q*', *M*, *N*, λ, a_0 and b_0 are material constants identified from large deformation tests. During firction stir welding there is a high deformation rate around the tool's pin and accordnigly Cho et al. [27] used an evolution equation to specify the strength's saturation value which is a function of temperature and strain rate. In their work *K* was also defined under a Voce-like saturation limit.

2.2.7 Dorfler emperical model

As strain values in material around tool during FSW is high and tension test gives limited strain value, the tensile test data may be suitable only to a limited extend for finding the parameters of a given constitutive model. To model the material behaviour under large deformations more precisely, an empirical material model was introduced by Dorfler [109] based on experimental data from torsion test.

Dorfler model: $\sigma(\dot{\varepsilon},T) = a_a + b_a T + c_a T^2 - a_b(T - b_b)\ln(\dot{\varepsilon} + a_c + b_c T + c_c T^2)$ (18)

σ is the flow stress, $\dot{\varepsilon}$ is the strain rate, T is the temperature and a_i, b_i, c_i are material constants. The empirical model factors have been worked out for strain hardened aluminum alloys as well as for precipitation hardened alloys and showed [109] good results for both alloy types. Dorfler [109] also compared his model with the Johnson-Cook constitutive model and showed that his model predictions are slightly lower compared to experimental stress-strain curves of two aluminum alloys, whereas the Johnson-Cook model results were quite higher compared to test data.

Hansel-Spittel is another constitutive model which has been used by Assidi et al. [56] in FSW modeling; however in that work the model generated a maximum temperature higher than the material melting point and hence they suggested the Norton-Hoff constitutive equation instead. There are other constitutive equations which have been developed in CSM approaches but have not, or rarely, been used in the FSW literature to date. These include: Bingham-Norton [132], Garvus [156], Zerilli-Armstrong (ZA) [157], Follansbee-Kocks (mechanical threshold stress model) [158], Mackawa [159], modified Johnson-Cook [160], Usui [161], Bammann-Chiesa-Johnson (BCJ) [162], Physics-based (PB) [163], Cowper-Symonds [164], Steinberg–Cochran–Guinan–Lund [165, 166] and Preston–Tonks–Wallace [167].

Finally, we would like to add that there are also some other equations for stress-strain response of materials, but the effect of strain rate is not considered in these models [168]:

Ludwik equation [169]: $\sigma = \sigma_0 + k\varepsilon^m$ (19)

Hollomon equation [170]: $\sigma = k\varepsilon^n$ (20)

Swift equation [171]: $\sigma = k(\varepsilon + \varepsilon_0)^n$ (21)

Voce equation [172]: $\sigma = B - (B - A)\exp(-n\varepsilon)$ (22)

Levy-Mises equation (also called flow rules) [173]: $\frac{d\varepsilon_1}{\sigma_1'} = \frac{d\varepsilon_2}{\sigma_2'} = \frac{d\varepsilon_3}{\sigma_3'} = d\lambda$ (23)

III. IMPLEMENTING AND COMPARING SELECTED CONSTITUTIVE EQUATIONS IN A SAME FSW MODEL

The integrated multiphysics FSW model considered for aluminum 6061 in the present work is adapted from [129], where details on different modules of the model can be found. In brief, the model uses a 2D Eulerian multiphysics flow formulation. We neglected the elastic behavior and strain hardening of the aluminum alloy as there is high strain during FSW; i.e. a perfectly vicoplastic deformation is considered without strain hardening and with fluid flow. The Perzyna viscosity law (Eq. 5) with the Zener-Hollomon flow stress equation (Eq. 10) and heat transfer equation were initially employed to model the flow stress of the material and provide the necessary temperature- and strain rate-dependent viscosity of the aluminum fluid. Also the Zener-Hollomon flow stress equation was used to define the pin heat flux. An empirical cut-off temperature (50 ^{o}C lower than solidus temperature) was applied to prevent temperature increase higher than solidus. The velocity boundary conditions are applied by defining a stick coefficient between the tool and workpiece. The model has been already validated using experimental data and other published models as discussed in [129]. The process conditions include a tool RPM of ω=186 and the weld speed of u_{weld}=2.34 mm/sec (Figure 4). In the next sections we aim to apply a set of selected constitutive equations reviewed in Section 2 to this FSW model of aluminum 6061 via the following implantations.

3.1 Applying different dynamic viscosity equations of aluminum 6061

As parameters of the dynamic viscosity equation of Carreau model (Eq 4) are reported in Atharifar et al. [117], and the Zener-Hollomon flow stress (Eq 10) model constants in Tello et al. [145], we used these two constitutive equations to develop Carreau and Perzyna dynamic viscosity (Eq. 5) models, respectively. Also the Zener-Hollomon flow stress was used to simulate the pin heat flux of the model, where we can predict temperature, shear strain rate, shear stress, viscosity and the applied torque around pin.

3.2 Identifying the power law viscosity model parameters for aluminum 6061

For comparison purposes, in the present work the power law dynamic viscosity model parameters (*m* and *n* in Eq. 1) were determined for aluminum 6061 near solidus by fitting the equation to Perzyna dynamic viscosity model response from [129] with the Zener-Hollomon flow stress. The fitted values of model parameters were $m=1.28\times10^{7}$ and $n=0.2$, with a coefficient of determination of $R^2=0.99$. As a result, the (CFD based) power law model was also considered in the pool of compared constitutive models.

3.3 Applying Johnson-Cook flow stress equations in Perzyna dynamic viscosity model

In order to study the effect of using Johnson-Cook flow stress equation (Eq 11) compared to Zener-Hollomon flow stress equation (Eq 10) on the resulting flow stress around pin, we applied the temperature, strain and strain rate distributions obtained by the Zener-Hollomon equation (under different viscosity laws) into the Johnson-Cook flow stress equation with the latter model constants taken from the work of Lesuer et al. [174] for aluminum 6061.
In the next section, we will first compare the effect of using different CFD based constitutive equations (namely, the power law, Carreau, and Perzyna models) with Zener-Hollomon flow stress model to simulate the pin heat flux. Next, we will compare the predicted shear stress values using the Zener-Hollomon and Johnson-Cook equations with the same temperature, shear strain rate and strain distributions around the pin found via each of the power law, Carreau and Perzyna viscosity models.

IV. RESULTS AND DISCUSSION

4.1 Effect of using different dynamic viscosity equations on CFD model results

The shear stress in the CFD model of FSW around the pin after using Perzyna, Carreau and power law dynamic viscosity equations are shown in Figure 4. In all the models in Figure 4 we use the Zener-Hollomon (ZH) flow stress to determine the tool's heat flux as discussed in [129]. It is clear that the three models resulted in a comparable flow stress around the pin, however Carreau model shows the lowest shear stress compared to the other two models.

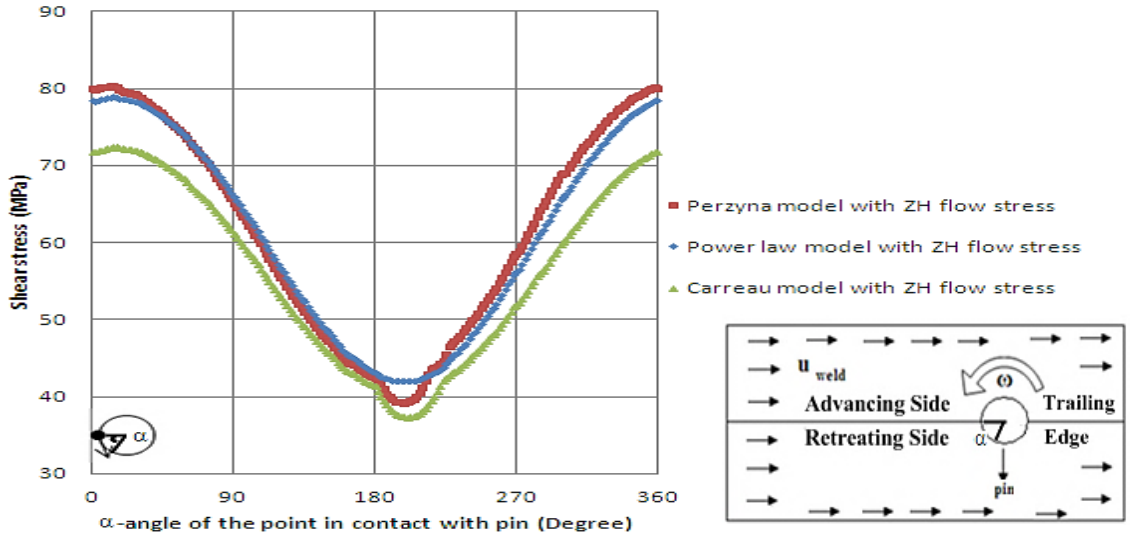

Figure 4: Effect of using different dynamic viscosity equations on shear stress around the pin

In Figure 5 the effect of different dynamic viscosity equations on the shear strain rate and temperature of points around the pin is shown. It is clear that the maximum temperature is somewhere between regions 2 and 3 and closer to region 3; i.e., in the trailing side of the pin (Figure 4) which is in agreement with earlier works [129]. Also the maximum shear rate occurs between regions 3 and 4 in advancing side of the plates. Apparently Carreau and power law models predict lower shear strain rates and temperature values compared to Perzyna dynamic viscosity model. Also they all result in a similar maximum temperature (about 540 ^{o}C) while the Carreau model predicts a slightly higher value.

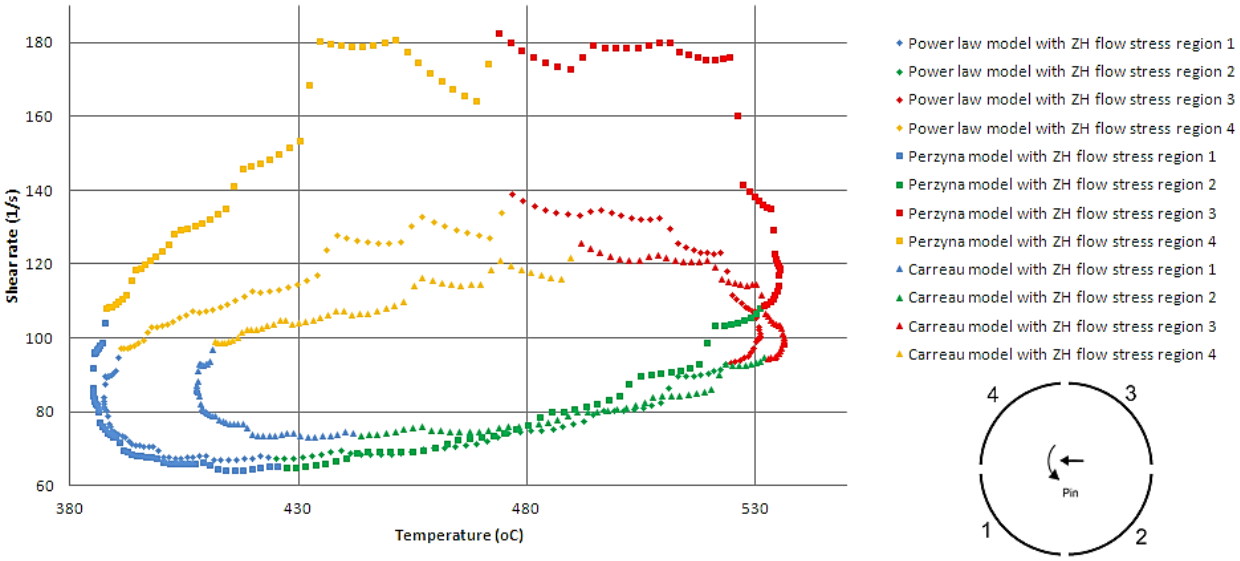

Figure 5: Effect of using different dynamic viscosity equations on shear strain rate and temperature around pin

Figure 6 shows that the effect of using different dynamic viscosity equations on resulting dynamic viscosity values around the pin is much more significant than the previous effects. Perzyna model with ZH flow stress predicts notably higher dynamic viscosity values compared to other dynamic viscosity models. Interestingly, however, they all show the same value at the point where the material temperature is equal to its solidus temperature. The difference in other regions would be due to the higher sensitivity of the Perzya constitutive model to temperature and shear stain rate changes around the pin.

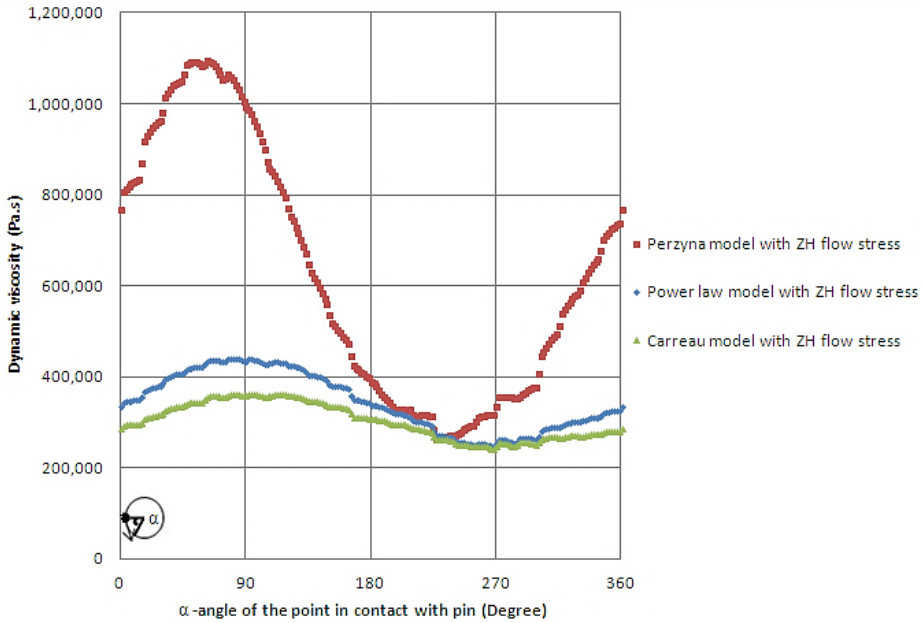

Figure 6: Effect of using different dynamic viscosity equations on dynamic viscosity around pin

We also compared the resulting temperature distribution on the weld line after using different dynamic viscosity models in the CFD model as shown in Figure 7. All of the models provided a very similar temperature distribution except for Carreau model at the leading edge (in front of the pin) which shows slightly higher temperatures.

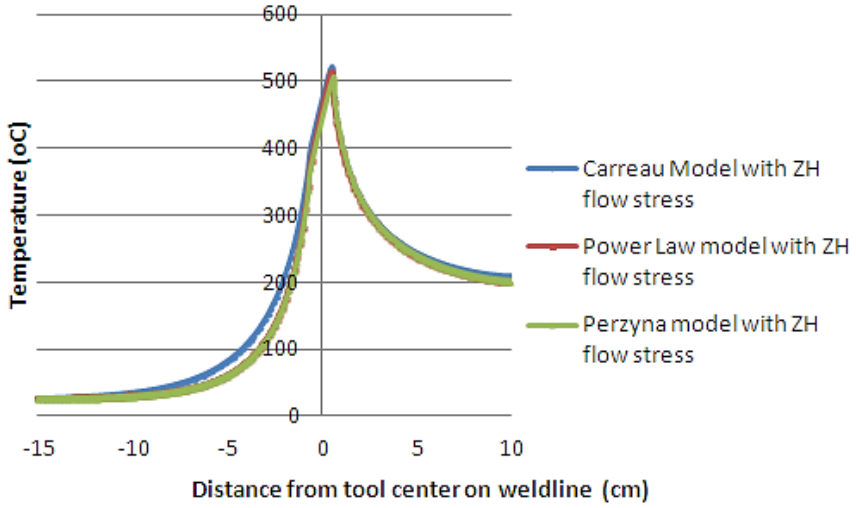

Figure 7: Effect of using different dynamic viscosity equations on maximum temperature on the weldline

Next, considering plates with 10 mm thickness, we calculated the resulting torque on the pin as shown in Figure 8. The predicted torque values are close to each other while in the Carreau model it is slightly lower compared to the other two dynamic viscosity models.

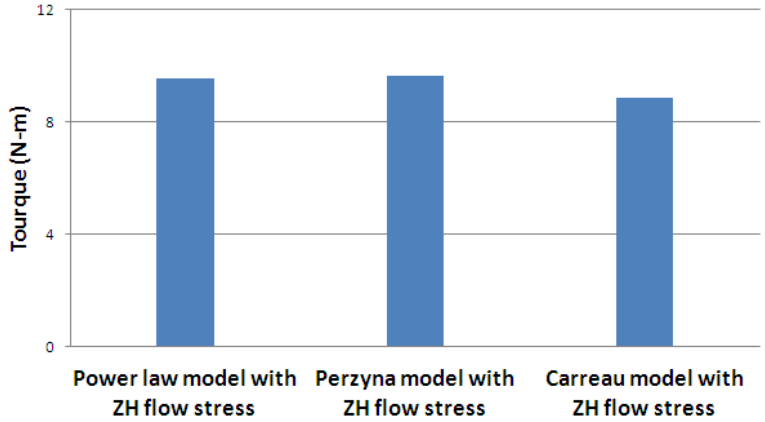

Figure 8: The Effect of using different dynamic viscosity equations in the CFD model on the predicted torque on the pin

4.2 Effect of using different CSM flow stress equations

In order to compare the Johnson-Cook (JC) flow stress model to the Zener-Hollomon (ZH) flow stress model under similar CFD viscosity laws (power law, Carreau or Perzyna), we obtained the temperature, strain and strain rate distributions resulted from Zener-Hollomon model with each of the above viscosity models and applied them into the JC flow stress equation for aluminum 6061. The results are shown in Figure 9 (data from Figure 4 have been added to Figure 9 for facilitating comparisons). As seen in Figure 9, using the JC flow stress model has resulted higher values of shear stress around the pin compared to the ZH flow stress model. Also when the JC model is used, the average value of shear stress around the pin is higher compared to that of the ZH model. This is because of high strain values during FSW around pin and its direct effect on the JC flow stress values, whereas the ZH flow stress is not strain dependant. This also suggests that the JC flow stress model may need some model tunings; for example an application of different stick coefficient may be required to use in the JC model for FSW simulations when compared to the ZH flow stress model.

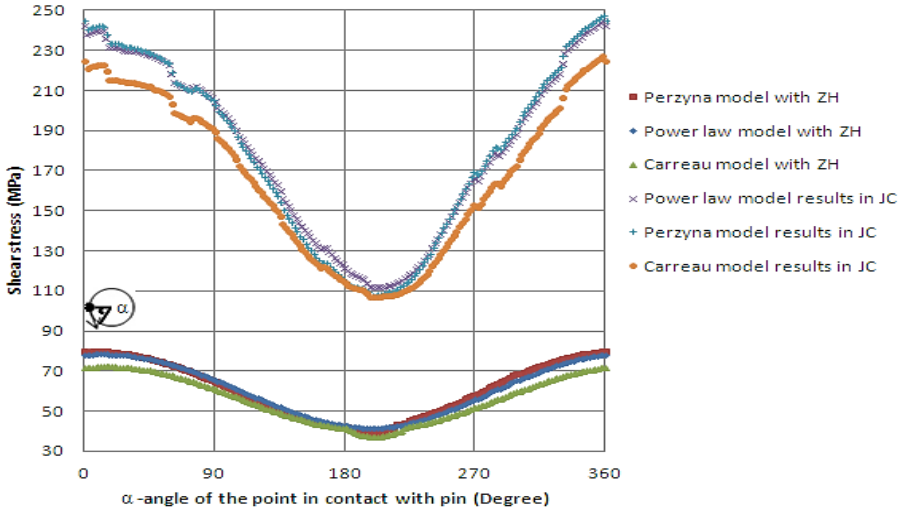

Figure 9: The effect of applying CFD model results (namely the temperature, strain and strain rate distributions) from ZH flow stress model into JC flow stress, under different dynamic viscosity equations

In order to understand exactly how much the deformation strains affects the JC flow stress model predictions, next we considered a strain state equal to zero around the pin by putting *B*=0 in Eq. 11 and applied the values of temperature and strain rate resulting from the CFD model with the ZH flow stress into the JC flow stress equation. The idea is that strain softening happens in high temperatures around the FSW tool by dynamic recrystallization and hence the strain values in this region are annihilated. The results of this attempt are shown in Figure 10.

It is clear that the shear flow stress resulted in the CFD model using the JC flow stress (elastoviscopolastic model) with zero strain around pin becomes much closer to the ones that had been resulted from the ZH flow stress model (perfectly viscoplastic), specially in the trailing edge (as shown in Figure 4). The 2D multiphysics model can be effectively used as a baseline to study the effect of other constitutive model parameters and understand their differences regarding model predictions and underlying material behaviours.

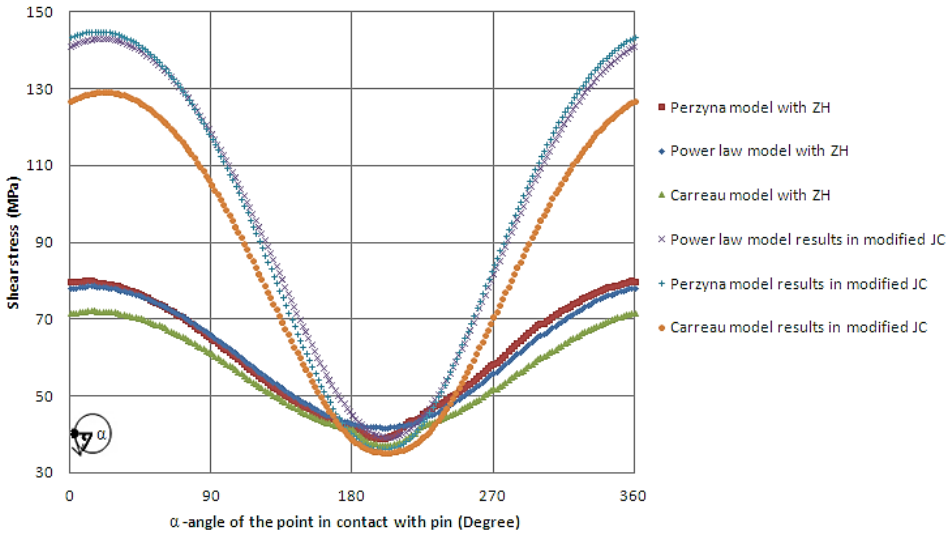

Figure 10: Effect of applying temperature and strain rate results from CFD model-ZH flow stress into the CSM-JC flow stress model, both under the condition of zero strain around the pin

V. CONCLUDING REMARKS

In this article, after a survey of earlier approaches, we studied the effect of using different constitutive equations in a previously validated multiphysics model of FSW, under the same welding conditions on aluminum 6061 sample. It was found that using the CFD approach, all the three dynamic viscosity equations (power law, Carreau model and Perzyna model) on average yielded similar shear stress

around the pin while the Carreau dynamic viscosity model predicted slightly lower values. Comparing the CFD and CSM approaches, however, it was found that if one uses the CFD approach's temperature, strain and strain rate predictions and import them into the Johnson-Cook flow stress equation (CSM approach), the resulting shear stress around the pin is in general much higher with the Johnson-Cook's flow stress equation compared to the Zener-Hollomon flow stress. Other specific results of the study may be summarized as follows.

- The maximum temperature occurs in the retailing edge of the pin (between regions 2 and 3 shown in Figure 3), while the maximum shear strain rate occurs in the advancing side of the pin (between regions 3 and 4) during FSW.
- All the three dynamic viscosity models (power law, Carreau model and Perzyna model) resulted in similar maximum temperatures, however the Carreau model predicts a relatively higher minimum temperature. Also Perzyna dynamic viscosity model generates higher shear strain rates compared to the power law and Carreau models.
- The dynamic viscosity in all the three CFD models becomes closer in the areas where temperature is near the solidus temperature of the plates. In other weld regions, the Perzyna dynamic viscosity model predicted higher dynamic viscosity values.
- The temperature distribution on the weld centerline and the required torque on the pin are predicted comparably using the three dynamic viscosity models. This means from a practical point of view, the external energy required to weld the material is independent of the underlying CFD constitutive models used for simulation.
- The Johnson-Cook (JC) flow stress equation may need a different FSW model tunings; for example applying a different stick coefficient, in order to predict a comparable model performance to the Perzyna dynamic viscosity model in FSW simulations. At high temperatures, if one drops the strain components from the JC model, it could predict shear stresses close to the ones predicted via the CFD dynamic viscosity equations with the Zener-Hollomon flow stress.

VI. FUTURE WORK

This study employed a 2D integrated multiphysics model of FSW for aluminum 6061 and compared the effect of different constitutive equations. For future studies, a 3D integrated multyphysics model can be developed for more accurate comparisons, in conjunction with more experimental data and in-situ weld studies, especially on FSW of thick plates or parts with irregular geometries. Other future work may include assessing the use other CSM and CFD based constitutive equations and their combinations; e.g., employing the Zener-Hollomon flow stress prediction in Perzyna dynamic viscosity model to predict FSW process outputs.

VII. ACKNOWLEDGMENT

The authors would like to acknowledge financial support from the Natural Sciences and Engineering Research Council (NSERC) of Canada.

REFERENCES

[1] Y.J. Chao, X. Qi, Thermal and thermo-mechanical modeling of friction stir welding of aluminum alloy 6061-T6, J. Mat. Process. Manuf. Sci. 7 (1998) 215–233.
[2] P. Dong, F. Lu, J.K. Hong, Z. Cao, Analysis of weld formation process in friction stir welding, Proceedings of the First International Conference on Friction Stir Welding, TWI, Thousand Oaks, 1999.
[3] A. Reynolds, X. Deng, T. Seidel, S. Xu, Recent advances in FSW process physics, Proceedings of the International Conference of Joining of Advanced and Specialty Materials, TWI, St. Louis, 2000.
[4] R.L. Goetz, K.V. Jata, Modeling friction stir welding of titanium and aluminum alloys, in: V. Jata, et al. (Eds.), Friction Stir Welding and Processing, TMS, Warrendale, 2001, pp. 35-42.
[5] A. Askari, S. Silling, B. London, M.W. Mahoney, Modeling and analysis of friction stir welding processes, in: V. Jata, et al. (Eds.), Friction Stir Welding and Processing, TMS, Warrendale, 2001, pp. 43-54.
[6] P. Dong, F. Lu, J.K. Hong, Z. Cao, Coupled thermomechanical analysis of friction stir welding process using simplified models, Sci. Technol. 6 (2001) 281-287.

[7] X. Deng, S. Xu, Solid mechanics simulation of friction stir welding process, Trans. NAMR–SME 29 (2001) 631–. 638.
[8] P. Heurtier, C. Desrayaud, F. Montheillet, A thermomechanical analysis of the friction stir welding process, Mat. Sci. Forum. 396-402 (2002) 1537–1542.
[9] S. Xu, X. Deng, Three-dimensional model for the friction-stir welding process. Theor. Appl. Mech. 21 (2002) 699-704.
[10] C.M. Chen, R. Kovacevic, Finite element modeling of friction stir welding-thermal and thermomechanical analysis, J. Mach. Tools Manuf. 43 (2003) 1319-1326.
[11] S. Guerdoux, L. Fourment, M. Miles, C. Sorensen, Numerical simulation of friction stir welding process using both Lagrangian and arbitrary Lagrangian Eulerian formulations, in: S. Ghosh, J.C. Castro, J.K. Lee (Eds.), Proceedings of Materials Processing and Design: Modeling, Simulation and Applications Conference, AIP, Columbus , 2004, pp. 1259-1264.
[12] C. Chen, R. Kovacevic, Thermomechanical modelling and force analysis of friction stir welding by the finite element method. J. Mech. Eng. Sci. 218 (2004) 509-519.
[13] L. Fourment, S. Guerdoux, M. Miles, T. Nelson, Numerical simulation of the friction stir welding process using both lagrangian and arbitrary lagrangian eulerian formulations, Proceedings of the Fifth International Conference on Friction Stir Welding, TWI, Metz, 2004.
[14] R.W. McCune, H. Ou, C.G. Armstrong, M. Price, Modelling friction stir welding with the finite element method: A Comparative Study, Proceedings of the Fifth International Conference on Friction Stir Welding, TWI, Metz, 2004.
[15] H. Schmidt, J. Hattel, Modelling thermomechanical conditions at the tool / matrix interface in Friction Stir Welding, Proceedings of the Fifth International Conference on Friction Stir Welding, TWI, Metz, 2004.
[16]X.K. Zhu, Y.J. Chao, Numerical simulation of transient temperature and residual stresses in friction stir welding of 304L stainless steel, J. Mat. Process. Tech. 146 (2004) 263-272.
[17] H.W. Zhang, Z. Zhang, J.T. Chen, The finite element simulation of the friction stir welding process, Mat. Sci. Eng.: A. 403 (2005) 340–348.
[18] H. Schmidt, J. Hattel, A local model for the thermomechanical conditions in friction stir welding, Modelling Simul. Mat. Sci. Eng. 13 (2005) 77-93.
[19] V. Soundararajan, S. Zekovic, R. Kovacevic, Thermo-mechanical model with adaptive boundary conditions for friction stir welding of Al 6061, Int. J. Mach. Tools Manuf. 45 (2005) 1577-1587.
[20] Z. Zhang, J.T. Chen, H.W. Zhang, Modeling of the friction stir process under different pressures on the shoulder, J. Aeronaut. Mat. 25 (2005) 33-37.
[21] D. Forrest, J. Nguyen, M. Posada, J. Deloach, D. Boyce, J. H. Cho, Simulation of HSLA-65 friction stir welding, Proceedings of the 7th International Conference on Trends in Welding Research, ASM, Pine Mountain, 2005.
[22] J. Hua, R. Shivpuri, L. Fratini, A continuum based fem model for friction stir welding—model development, Mat. Sci. Eng. A, 419 (2006) 389-396.
[23] H.W. Zhang, Z. Zhang, J. Bie, L. Zhou, J. Chen, Effect of viscosity on material behavior in friction stir welding process, Trans. Nonferrous Met. SOC. China. 16(2006) 1045-1052.
[24] G. Buffa, L. Fratini, J. Hua, R. Shivpuri, Friction stir welding of tailored blanks: investigation on process feasibility, Annals of the CIRP. 55 (2006) 2-5.
[25] G. Buffa, J. Hua, R. Shivpuri, L. Fratini, Design of the friction stir welding tool using the continuum based FEM model, Mat. Sci. Eng. A. 419 (2006) 381-388.
[26] P. Heurtier, M.J. Jones, C. Desrayaud, J. H. Driver, F. Montheillet, D. Allehaux, Mechanical and thermal modelling of friction stir welding, J. Mat. Proc. Technol. 171 (2006) 348-357.
[27] J.H. Cho, P.R. Dawson, Investigation on texture evolution during friction stir welding of stainless steel, Metall. Mat. Trans. A. 37(2006) 1147-1164.
[28] Z. Zhang, H.W. Zhang, Material behaviors and mechanical features in friction stir welding process, Inter. J. Adv. Manuf. Technol. 35 (2007) 86-100.
[29] H.W. Zhang, Z. Zhang, J.T. Chen, 3D modeling of material flow in friction stir welding under different process parameters, J. Mat. Process. Technol. 183 (2007).62-70.
[30] Z. Zhang, H.W. Zhang, Numerical studies on effect of axial pressure in friction stir welding, Sci. Technol. Weld. Join. 12 (2007) 226-249.
[31] D. Jacquin, C. Desrayaud, F. Montheillet, A thermo-fluid analysis of the friction stir welding process, Mat. Sci. Forum, 539-543 (2007) 3832-3837.
[32] J.H. Cho, S.H. Kang, K. Hwan Oh,. H.N.Han, S.B. Kang, Friction stir weld modeling of aluminum alloys, Adv. Mat. Research. 26-28 (2007) 999-1002.
[33] Y. He, D.E. Boyce, P.R. Dawson, Three-dimensional modeling of void growth in friction stir welding of stainless steel, Proceedings of the Materials Processing and Design: Modeling, Simulation and Applications Conference, AIP, Porto, 2007.

[34] J.H. Cho, H.W. Kim, S.B. Kang, Overview of modeling strength evolution during friction stir welding, Mat. Sci. Forum. 575-78 (2008) 805-810.
[35] J.H. Cho, P.R. Dawson, Modeling texture evolution during friction stir welding of stainless steel with comparison to experiments, J. Eng. Mat. Technol. 130 (2008) 1-12.
[36] Y. He, P.R. Dawson, D.E. Boyce, Modeling damage evolution in friction stir welding process, J. Eng. Mat. Technol. 130 (2008) 1-10.
[37] A. Bastier, M.H. Maitournam, F. Roger, K.D. Van, Modelling of the residual state of friction stir welded plates, J. Mat. Process. Technol. 200 (2008) 25–37.
[38] Z. Zhang, H.W. Zhang, Simulation of 3D material flow in friction stir welding of AA6061-T6, China Weld. 17 (2008) 57-63.
[39] G. Buffa, L. Fratini, R. Shivpuri, Finite element studies on friction stir welding processes of tailored blanks, Compu. Struct. 86 (2008) 181-189.
[40] H. Li, D. Mackenzie, Coupled thermo-mechanical modelling of friction stir welding, Proceedings of ASME Pressure Vessels and Piping Division Conference, ASME, San Antonio, 2008.
[41] Z. Zhang, H.W. Zhang, A fully coupled thermo-mechanical model of friction stir welding, Inter. J. Adv. Manuf. Technol. 37(2008) 279-293.
[42] H.B. Schmidt, J.H. Hattel, A thermal-pseudo-mechanical model for the heat generation in Friction Stir Welding, Scrip. Mat. 58 (2008) 332–337.
[43] O. Lorrain, V. Favier, H. Zahrouni, M.E. Hadrouz, A critical analysis of FSW simulations, Proceedings of 7th International Friction Stir Welding Symposium, TWI, Awaji Island, 2008.
[44] G. Buffa, L. Fratini, S. Pasta, R. Shivpuri, On the thermo-mechanical loads and the resultant residual stresses in friction stir processing operations, Mat, Sci. Eng. A. 57 (2008). 287-290.
[45] L. Fratini, G. Buffa, Metallurgical phenomena modeling in friction stir welding of aluminium alloys: analytical versus neural network based approaches, J. Eng. Mat. Technol. 130 (2008) 1-6.
[46] Z. Zhang, H.W. Zhang, Numerical studies on the effect of transverse speed in friction stir welding, Mat. Design. 30 (2009) 900-907.
[47] G. Buffa, G. Campanile, L. Fratini, A. Prisco, Friction stir welding of lap joints: Influence of process parameters on the metallurgical and mechanical properties, Mat. Sci. Eng. A. 519 (2009) 19-26.
[48] M. Grujicic, T. He, G. Arakere, , H.V. Yalavarthy, C.F. Yen, B.A. Cheeseman, Fully coupled thermomechanical finite element analysis of material evolution during friction-stir welding of AA5083, J. Eng. Manuf. 224 (2009) 609-625.
[49] Z. Zhang, H.W. Zhang, Numerical studies on controlling of process parameters in friction stir welding, J. Mat. Proc. Technol. 209 (2009) 241-270.
[50] L. Fratini, G. Buffa, D. Palmeri, Using a neural network for predicting the average grain size in friction stir welding, processes. Comput. Struc., 87 (2009) 1166-1174.
[51] J. Gagner, A. Ahadi, Finite element simulation of an AA2024-T3 friction stir weld, Inter. Rev. Mech. Eng. 3 (2009) 427-436.
[52] G. Buffa, L. Fratini, B. Arregi, M. Penalva, A new friction stir welding based technique for corner fillet joints: experimental and numerical study, Int. J. Mat. Form. 3 (2010) 1039-1042.
[53] R. Hamilton, D. MacKenzie, H. Li, Multi-physics simulation of friction stir welding process, Int. J. Comp. Aid. Eng. Soft. 27 (2010) 967-985.
[54] S. Mukherjee, A. Ghosh, Flow visualization and estimation of strain and strain-rate during friction stir process, Mat. Sci. Eng.: A. 527(2010) 5130-5135.
[55] F. Gemme, Y. Verreman, L. Dubourg, M. Jahazi, Numerical analysis of the dwell phase in friction stir welding and comparison with experimental data, Mat. Sci. Eng. A. 527 (2010) 4152-4160.
[56] M. Assidi, L. Fourment, S. Guerdoux, T. Nelson, Friction model for friction stir welding process simulation : Calibrations from welding experiments, Inter. J. Mach. Tool. Manuf. 50 (2010) 143-155.
[57] T. Azimzadegan, S. Serajzadeh, Thermo-mechanical modeling of friction stir welding, Int. J. Mat. Res. 101 (2010) 390-397.
[58] G.A. Moraitis, G.N. Labeas, Investigation of friction stir welding process with emphasis on calculation of heat generated due to material stirring, Sci. Technol. Weld. Join. 15 (2010) 177-184.
[59] P.F. Mendez, K.E. Tello, T.J. Lienert, Scaling of coupled heat transfer and plastic deformation around the pin in friction stir welding, Act. Mat. 58 (2010) 6012-6026.
[60] C.C. Tutum, J.H. Hattel, A multi-objective optimization application in friction stir welding: considering thermo-mechanical aspects, Proceedings of IEEE World Congress on Computational Intelligence and Congress on Evolutionary Computation, IEEE, Barcelona, 2010.
[61] K.L. Nielsen, T. Pardoen, V. Tvergaard, B. D. Meester, A. Simar, Modelling of plastic flow localisation and damage development in friction stir welded 6005A aluminium alloy using physics based strain hardening law, Int. J. Solid. Struct. 47 (2010) 2359-2370.

[62] M. Grujicic, G. Arakere, H. V. Yalavarthy, T. He, C. Yen, B.A. Cheeseman, Modeling of AA5083 material-microstructure evolution during butt friction-stir welding, J. Mat. Eng. Perform. 19 (2010) 672-684.
[63] H. Jamshidi Aval, S. Serajzadeh, A.H. Kokabi, Theoretical and experimental investigation into friction stir welding of AA 5086, Int. J. Adv. Manuf. Technol. 52 (2011) 531-544.
[64] D. Jacquin, B.D. Meester, A. Simar, D. Deloison, F. Montheillet, C. Desrayaud, A simple Eulerian thermomechanical modeling of friction stir welding, J. Mat. Process. Technol, 211 (2011) 57-65.
[65] G. Buffa, A. Ducato, L. Fratini, Numerical procedure for residual stresses prediction in friction stir welding, Finit. Elem. Analy. Design. 47 (2011) 470-476.
[66] M. Grujicic, B. Pandurangan, C. Yen, B.A. Cheeseman, Modifications in the AA5083 Johnson-Cook material model for use in friction stir welding computational analyses, J. Mat. Eng. Perform. 21 (2012). 2207-2217.
[67] A. Simar, Y. Bréchet, B. De Meester, A. Denquin, C. Gallais, T. Pardoen, Integrated modeling of friction stir welding of 6xxx series Al alloys: Process, microstructure and properties, Progress Mat. Sci. 57 (2012) 95-183.
[68] G.J. Bendzsak, T. North, C. Smith, An experimentally validated 3D model for friction stir welding, Proceedings of the 2nd International Symposium on Friction Stir Welding, TWI, Gothenburg, 2000.
[69] P.A. Colegrove, M. Painter, D. Graham, T. Miller, 3 dimensional flow and thermal modeling of the friction stir welding process, Proceedings of the 2nd International Symposium on Friction Stir Welding, TWI, Gothenburg, 2000.
[70] P. Ulysse, Three-dimensional modeling of the friction stir-welding. *Process Int. J. Mach. Tools. Manuf.*, *42* (2002) 1549-1557.
[71] H.R. Shercliff, P.A. Colegrove, Modelling of friction stir welding, Proceddings of the Mathamathical Modeling of Weld Phenomenon 6 Conference, Maney, Graz, 2002.
[72] A. P. Reynolds, K. Linder, W. Tang, T.U. Siedel, Weld efficiency and defect formation correlation between experiment and simple models, Proceedings of the 6th International Trends in Welding Research Conference, ASM, Pine Mountain, 2003.
[73] A. P. Reynolds, M.Z.H. Khandkar, T. Long, W. Tang, J.A. Khan, Utility of relatively simple models for understanding process parameter effects on FSW, Mat. Sci. Forum. 426·432 (2003) 2959-2694
[74] P.A. Colegrove, H.R. Shercliff, Experimental and numerical analysis of aluminium alloy 7075-T7351 friction stir welds, Sci. Technol. Weld. Join. 8 (2003) 360-368.
[75] T.U. Seidel, A.P. Reynolds, Two-dimensional friction stir welding process model based on fluid mechanics, Sci. Technol. Weld. Join. 8 (2003). 175-183.
[76] P.A. Colegrove, H.R. Shercliff, Development of Trivex friction stir welding tool part 1– two-dimensional flow modelling and experimental validation, Sci. Technol. Weld. Join. 9 (2004) 345-351.
[77] P.A. Colegrove, H.R. Shercliff, Development of Trivex friction stir welding tool part 2 – three-dimensional flow modelling, Sci. Technol. Weld. Join. 9 (2004) 352-362.
[78] D. Schmitter, I.M. Zylla, Modelling friction stir welding with thermally coupled fluid dynamics, J. Phys. 120 (2004) 677-680
[79] P.A. Colegrove, Modeling and development of the Trivex friction stir welding tool, Weld. World. 48 (2004) 10-26.
[80] P.A. Colegrove, H.R. Shercliff, 2-Dimensional CFD modelling of flow round profiled FSW tooling. Sci Technol. Weld. Join. 9 (2004) 483-492.
[81] P.A. Colegrove, H.R. Shercliff, Modelling the friction stir welding of aerospace alloys, Proceedings of the 5th International Symposium on Friction Stir Welding, TWI, Metz, 2004.
[82] S. Hirasawa, K. Okanoto, S. Hirano, T. Tomimura, Analysis of flow and temperature distribution during friction stir welding, Proceedings of ASME Heat Transfer/Fluids Engineering Summer Conference, ASME, Charlotte, 2004.
[83] H. Schmidt, J. Hattel, CFD modelling of the shear layer around the tool probe in friction stir welding, Proceedings of Friction Stir Welding and Processing III, TMS, San Francisco, 2005.
[84] P.A. Colegrove, H.R. Shercliff, 3-Dimensional CFD modelling of flow round a threaded friction stir welding tool profile, J. Mat. Process. Technol. 169 (2005) 320-327.
[85] R. Nandan, G.G. Roy, T.J. Lienert, T. Debroy, Numerical modelling of 3D plastic flow and heat transfer during friction stir welding of stainless steel, Sci Technol. Weld. Join. 11 (2006) 526-537.
[86] R. Nandan, G. Roy, Numerical simulation of three-dimensional heat transfer and plastic flow during friction stir welding, Metall. Mat. Trans. A. 37 (2006) 1247-1259.
[87] A. Bastier, M.H. Maitournam, K.D. Van, F. Roger, Steady state thermomechanical modelling of friction stir welding, Sci Technol. Weld. Join. 11 (2006) 278-288.
[88] R. Crawford, G.E. Cook, A.M. Strauss, A.C. Nunes, A mechanistic study of the friction stir welding process, Proceedings of the 57th International Astronautical Congress, IAF, Valencia, 2006

[89] E. Foulvarcit, Y. Gooroociturn, F. Boltout, 3D Modelling of Thermofluid Flow in Friction Stir Welding, Proceedings of the 7th International Conference on Trends in Welding Research, ASM, Pine Mountain, 2006.
[90] R. Crawford, G.E. Cook, A.M. Strauss, D.A. Hartman, M.A. Stremler, Experimental defect analysis and force prediction simulation of high weld pitch friction stir welding, Sci Technol. Weld. Join. 11 (2006) 657-665.
[91] T. Long, A.P. Reynolds, Parametric studies of friction stir welding by commercial fluid dynamics simulation, Sci Technol. Weld. Join. 11 (2006) 200-208.
[92] H. Schmidt, J. Hattel, Analysis of the velocity field in the shear layer in FSW: experimental and numerical modelling, Proceedings of 6th International Friction Stir Welding Symposium, TWI, Saint Sauveur, 2006.
[93] T. Sato, D. Otsuka, Y. Watanabe, R.S. Division, N. Sharyo Designing of friction stir weld parameters with finite element flow simulation, Proceedings of 6th International Friction Stir Welding Symposium, TWI, Saint Sauveur, 2006.
[94] C.B. Owen, Two dimensional friction stir welding model with experimental validation. Master's Thesis, Brigham Young University, 2006.
[95] A.M. Tartakovsky, G. Grant, X. Sun, S.T. Hong, M. Khaleel, Smooth particle hydrodynamics (sph) model for friction stir welding (fsw) of dissimilar materials, Proceedings of 6th International Friction Stir Welding Symposium, TWI, Saint Sauveur, 2006.
[96] P.A. Colegrove, H.R. Shercliff, CFD modelling of friction stir welding of thick plate 7449 aluminium alloy, Sci Technol. Weld. Join. 11(2006), 429-441.
[97] R. Crawford, T. Bloodworth, G.E. Cook, A.M. Strauss, D.A. Hartman, High speed friction stir welding process modeling, Proceedings of 6th International Friction Stir Welding Symposium, TWI, Saint Sauveur, 2006.
[98] T.D. Vuyst, O. Magotte, A. Robineau, J.C. Goussain, L. D'Alvise, Multi-physics simulation of the material flow and temperature field around FSW tool, Proceedings of the Sixth International Conference on Friction Stir Welding, TWI, Montreal, 2006.
[99] I. Alfaro, L. Fratini, E. Cueto, F. Chinesta, F. Micari, Meshless simulation of friction stir welding. Proceedings of the Materials Processing and Design: Modeling, Simulation and Applications Conference, AIP, Porto, 2007.
[100] T. De Vuyst, , & L.D Alvise, Material flow around a friction stir welding tool: development of a thermo-fluid code, Weld. World. 51 (2007) 37-43.
[101] H. Chen, Y. Zhao, Y. Zhang, L. Wu, S. Lin, , Mechanistic study on friction stir welding of 2014 aluminium alloy, Proceeding of 58th International Astronautical Congress, IAF/IAA, Hyderabad, 2007.
[102] H. Atharifar, D.C. Lin, , R. Kovacevic, Studying tunnel-like defect in friction stir welding process using computational fluid dynamics, Proceedings of Materials Science & Technology Conference and Exhibition: Exploring Structure, Processing, and Applications Across Multiple Materials Systems, Detroit, 2007
[103] L. St-Georges, V. Dassylva-Raymond, L.I. Kiss, A.L. Perron, Transport phenomena in Friction Stir Welding, Proceedings of friction stir welding and processing IV, TMS, Orlando, 2007.
[104] P.A. Colegrove, H.R. Shercliff, R. Zettler, Model for predicting heat generation and temperature in friction stir welding from the material properties, Sci Technol. Weld. Join. 12 (2007) 284-297.
[105] T. Long, W. Tang, A.P. Reynolds, Process response parameter relationships in aluminium alloy friction stir welds, Sci Technol. Weld. Join. 12 (2007) 311-317.
[106] R. Nandan, , G.G. Roy, T. J. Lienert, T. Debroy, Three-dimensional heat and material flow during friction stir welding of mild steel, Acta Material. 55 (2007) 883-895.
[107] R. Nandan, B. Prabu, A. De, T. Debroy, Improving reliability of heat transfer and materials flow calculations during friction stir welding of dissimilar aluminum alloys, Weld. Research. 86 (2007) 313-322.
[108] H. Atharifar, R. Kovacevic, Numerical study of the tool rake angle effect on the material flow in friction stir welding process, Proceedings of IMECE2007 ASME international Mechanical Engineering Congress and Exposition, ASME, Seattle, 2007.
[109] S.M. Dörfler, Advanced modeling of friction stir welding – improved material model for aluminum alloys and modeling of different materials with different properties by using the level set method, Proceedings of the COMSOL 2008 Conference, COMSOL, Hannover, 2008.
[110] L. St-georges, L.I. Kiss, V. Dassylva-Raymond, Mixing mechanism in friction stir welding of metallic composites, Proceedings of 7th International Friction Stir Welding Symposium, TWI, Awaji Island, 2008.
[111] B.C. Liechty, B.W. Webb, Modeling the frictional boundary condition in friction stir welding., Int. J. Mach. Tool. Manuf. 48 (2008) 1474- 1485.
[112] H. Schmidt, Thermal and material flow modelling of friction stir welding using Comsol, Proceedings of the COMSOL Conference, COMSOL, Hanover, 2008.

[113] R. Nandan, T.J. Lienert, , T. Debroy, Toward reliable calculations of heat and plastic flow during friction stir welding of TI-6AL-4V alloy, Int. J. Mat. Res. 99 (2008) 434-444.
[114] A. Kumar, D.P. Fairchild, S.J. Ford, Modeling of heat transfer and material flow during FSW of steel, Proceedings of 7th International Friction Stir Welding Symposium, TWI, Awaji Island, 2008.
[115] D. Kim, H. Badarinarayan, K. Chung, Thermo-mechanical modeling of friction stir butt welding process of AA5083-H18- CFD modeling with steady state description, Proceedings of 7th International Friction Stir Welding Symposium, TWI, Awaji Island, 2008.
[116] D.H. Lammlein, D.R. DeLapp, P.A. Fleming. A.M. Strauss, G.E. Cook, The application of shoulderless conical tools in friction stir welding: An experimental and theoretical study, Mat. Design. 30 (2009) 4012-4022.
[117] H. Atharifar, D. Lin, R. Kovacevic, Numerical and Experimental Investigations on the Loads Carried by the Tool During Friction Stir Welding, J. Mat. Eng. Perform. 18 (2009) 339-350.
[118] A. Arora, Z. Zhang, A. De, T. Debroy, Strains and strain rates during friction stir welding, Scrip. Mat. 61 (2009) 863-866.
[119] D. Kim, H. Badarinarayan, J. Hoon, C. Kim, K. Okamoto, R.H. Wagoner, Numerical simulation of friction stir butt welding process for AA5083-H18 sheets. Europ. J. Mech./A Solid. 29 (2010) 204-215.
[120] J. Hilgert, H. Schmidt, J.F. Santos, N. Huber, (2010). Moving geometry process model for bobbin Tool FSW, Proceedings of 8th International Friction Stir Welding Symposium, TWI, Timmendorfer Strand, 2010.
[121] O.C. Zienkiewicz, P.C. Jain, E. Onate, Flow of solids during forming and extrusion- some aspects of numerical solutions, Int. J. Solids. Struct. 14 (1978) 15-38.
[122] A. Bastier, M.H. Maitournam, K.D. Van, F. Roger, Steady state thermomechanical modelling of friction stir welding. Sci. Technol. Weld. Join. 11 (2006) 278-289.
[123] A. Bastier, M.H. Maitournam, F. Roger, K.D. Van, Modelling of the residual state of friction stir welded plates, J. Mat. Process. Technol. 200 (2008) 25-37.
[124] T. De Vuyst, V. Madhavan, B. Ducoeur, A. Simar, B.D. Meester, L.D. Alvise, A thermo-fluid/ thermo-mechanical modelling approach computing temperature cycles and residual stresses in FSW, Proceedings of the 8th International Conference on Trends in Welding Research, ASM, Pine Mountain, 2008.
[125] X. Qin, P. Michaleris, Themo-elasto-viscoplastic modelling of friction stir welding, Sci. Technol. Weld. Join. 14 (2009) 640-649.
[126] M. Nourani, A.S. Milani, S. Yannacopoulos, C.Y. Yan, Predicting residual stresses in friction stir welding of aluminum alloy 6061 using an integrated multiphysics model, Proceedings of the 9th International Conference on Residual Stresses (ICRS 9), Garmisch-Partenkirchen , 2012.
[127] B.A.B. Andersson, Thermal stress in a submerged-arc welded joint considering phase transformations, J. Eng. Mater. Technol. 100 (1978) 356-362
[128] V.J. Papazoglou, K. Masubuchi, Numerical analysis of thermal stresses during welding including phase transformation effects, J. Press. Vessel Technol. 104 (1982) 198-203.
[129] M. Nourani, A. S. Milani (Ed.), S. Yannacopoulos (Ed.), Friction Stir Welding of Aluminum Alloys, OmniScriptum GmbH & Co. KG, Saarbrücken,, 2014.
[130] M. Nourani, A.S. Milani, S. Yannacopoulos, C. Yan, Predicting grain size distribution in friction stir welded 6061 aluminum alloy, Proceedings of 9th International Friction Stir Welding Symposium, TWI, Huntsville, 2012.
[131] R. Darby, Chemical Engineering Fluid Dynamics, second ed., CRC, New York, 2001.
[132] F. Irgens, Continuum Mechanics, reprint, Springer, 2008.
[133] P. Perzyna, Fundamental problems in visco-plasticity, in: Recent Advances in Applied Mechanics, Academic Press, New York,1966.
[134] O.C. Zienkiewicz, I.C. Cormeau, Visco-plasticity. plasticity and creep in elastic solids: a unified numerical solution approach, Int. J Num. Meth. Eng. 8 (1974) 821-845.
[135] K. Kuykendall, C. Sorensen, T. Nelson, (2011). A comparison of experimental data and model predictions with constitutive laws commonly used to model friction stir welding, Proceedings of Friction Stir Welding and Processing V Conference, John Wiley & Sons Inc., Hoboken, 2011.
[136] PJ. Carreau, Rheological equations from molecular network theories, Trans Soc Rheol. 16 (1972) 99-127.
[137] G.J. Bendzsak, T.H. North, Z. Li , Numerical model for steady state flow in friction welding, Acta. Mater. 45 (1997) 1735-1745.
[138] G.J. Bendzsak, T.H. North, Numerical modelling of fluid dynamics and heat transfer in friction welding, Proceedings of Mathematical Modelling of Weld Phenomena 4, Institute of Materials, London, 1998.
[139] T.C. Papanastasiou, Flows of materials with yield, J. Rheo. 31(1987) 385-390.
[140] J.C. Simo, T.J.R. Hughes, Computational inelasticity: Interdisciplinary Applied Mathematics, Springer-Verlag, New York, 1998.

[141] F. Humphreys, M. Hatherly, Recrystallization and Related Annealing Phenomena, second ed., Elsevier, Oxford, 2004.
[142] C. Zener, J.H. Hollomon, Effect of strain rate upon plastic flow of steel, J. App. Phys. 15 (1944) 22-32.
[143] C.M. Sellars, W.J.McG. Tegart, Hot workability, Int. Met. Rev., 17 (1972) 1-24.
[144] T. Sheppard, D.S. Wright, Determination of flow stress: Part 1 constitutive equation for aluminum alloys at elevated temperatures, Met. Technol. 6 (1979) 215-223.
[145] K. Tello, A. Gerlich, P. Mendez, Constants for hot deformation constitutive models for recent experimental data, Sci. Technol. Weld. Join. 15(2010) 260–266.
[146] R.G. Johnson, W. H. Cook, A constitutive model and data for metals subjected to large strains, high strain rates and high temperatures. Proceedings of International Symposium on Ballistics, ADPA, Hague, 1983.
[147] J.L. Chenot, M. Bellet, The viscoplastic approach for the finite element modeling of metal forming precosses, in: P Hartley, I Pillinger and C Sturgess (Eds.) Numerical modelling of material deformation precosses, Springer-Verlag, 1992, 179-224.
[148] R.H. Wagoner, J.L. Chenot, Metal Forming Analysis, Cambridge University Press, New York, 2001.
[149] H, Mecking, U.F. Kocks, Kinetics of flow and strain-hardening, Acta Metal. 29 (1981) 1865–75.
[150] Y. Estrin, H. Mecking A unified phenomenological description of work hardening and creep based on one-parameter models, Acta Metal. 32 (1984) 57–80.
[151] U.F. Kocks, H. Mecking, Physics and phenomenology of strain hardening: the FCC case, Prog. Mater. Sci. 48 (203) 171–273.
[152] E. Voce, Practical strain-hardening function, Acta Metal. 51 (1955) 219-26.
[153] E.W. Hart, Constitutive relations for the nonelastic deformation of metals, J. Eng. Mater. Technol. 98 (1976) 193-202.
[154] G. Eggert, P. Dawson, On the use of internal variable constitutive equations in transient forming processes, Int. J. Mech. Sci. 29 (1987) 95-113.
[155] G. Eggert, P. Dawson, A viscoplastic formulation with elasticity for transient metal forming, Comput. Meth. Appl. Mech. Eng. 70 (1988) 165-90.
[156] A. Garvus, Formulation of a new constitutive equation available simultaneously for static and dynamic loading. Proceedings of the 9th International Conference on the Mechanical and Physical Behaviour of materials under Dynamic Loading, DYMAT, Brussels, 2009.
[157] F.J. Zerilli, R.W. Armstrong, Dislocation-mechanics-based constitutive relations for material dynamics calculations, J. App. Phys. 61 (1987)1816-1825.
[158] P.S. Follansbee, U.F. Kocks, A constitutive description of the deformation of copper based on the use of the mechanical threshold, Acta Metal. 36 (1988) 81–93.
[159] Private communication between Maekawa and Childs as appeared in Childs, T. H. C, Material Property Requirements for Modeling Metal Machining, 1997, Colloque C3, Journal de physique, III: XXI–XXXIV.
[160] U.R. Andrade, M.A. Meyers, K.S. Vecchio, A.H. Chokshi, Dynamic recrystallization in high-strain, high-strain-rate plastic deformation of copper, Acta Metal. et Mater. 42 (1994) 3183–95.
[161] K. Maekawa, T. Shirakashi, E. Usui, Flow stress of low carbon steel at high temperature and strain rate (Part 2), Bull. Jap. Soc. Precis. Eng. 17 (1983) 167-72.
[162] D.J. Bammann, M.L. Chiesa, G.C. Johnson, Modeling large deformation and failure in manuf. processes, Proceedings of Theoretical and Applied Mechanics Conference, Kyoto, 1996.
[163] S. Nemat-Nasser, J.B. Isaacs. Direct measurement of isothermal flow stress of metals at elevated temperatures and high strain rates with application to Ta and Ta–W alloys. Acta Mater. 45 (1997) 907-19.
[164] N. Jones, Structural Impact. Cambridge University Press, Cambridge, 1989.
[165] D.J. Steinberg, S.G. Cochran, M.W. Guinan, A constitutive model for metals applicable at high-strain rate, J. Appl. Phys. 51 (1980) 1498-1504.
[166] D.J. Steinberg, C.M. Lund, A constitutive model for strain rates from $10^{-4}$to 10^{6} s−1, J. Phys. Colloq. 49 (1988) 3-3.
[167] D.L. Preston, D.L. Tonks, D.C. Wallace, Model of plastic deformation for extreme loading conditions, J. Appl. Phys. 93 (2003) 211-220.
[168] H.J. Kleemola, M.A. Nieminen, On the strain-hardening parameters of metals, Metall. Trans. 5 (1974) 1863-1866.
[169] P. Ludwik, Elemente der Technologischen Mechanik, Verlag von Julius, Springer, Berlin, 1909.
[170] J.H. Hollomon, Tensile deformation, Trans. AIME, 162 (1945) 268-90.
[171] H.W. Swift, Plastic instability under plane stress, J. Mech. Phys. Solid. 1 (1952) 1-18.
[172] E. Voce, The relationship between stress and strain for homogeneous. deformation, J. Inst. Metal. 74 (1948) 537-62.
[173] Z. Marcinia, J.L. Duncan, S.J. Hu, Mechanics of Sheet Metal Forming, Butterworth-Heinemann, London, 2002.

[174] D.R. Lesuer, G. Kay, M. LeBlanc, Modeling large-strain, high-rate deformation in metals. Proceedings of the 3rd Biennial Tri-Laboratory Engineering Conference on Modeling and Simulation, Pleasanton, 1999.

AUTHORS BIOGRAPHY

M. Nourani received his PhD of Mechanical Engineering in 2013 from the University of British Columbia and his MSc and BSc from Sharif University of Technology in 2001 and 1999, respectively (all with honors). He has more than 10 years of work experience in R&D and design departments of automotive/trucking industry as well as more than 5 years in academy at different materials/mechanical labs and projects. His general expertise falls in the areas of CFD and CSM modeling, design, simulation & optimization of engineering materials, structures, and forming processes.

A. S. Milani joined the School of Engineering at the University of British Columbia Okanagan in 2007. He is currently Associate Professor of Mechanical Engineering and the leader of the Composites Research Network-Okanagan node. He was an NSERC (Natural Sciences and Engineering Research Council of Canada) fellow at the Massachusetts Institute of Technology (MIT) from 2005-2007. He received his PhD in 2005 from McGill University and his expertise falls in multi-scale modeling, simulation, and multi-criteria optimization of advanced engineering materials, structures, and forming processes.

S. Yannacopoulos joined UBC, Okanagan Campus, in 2006 as the Associate Dean and Director of the School of Engineering. Following his engineering education at the University of Manitoba, Ph.D. in Materials Science in 1986, he moved to the University of Saskatchewan where he advanced through the ranks, served as Head of Mechanical Engineering and Associate Dean and maintained an active research program in the area of Materials Science and Metallurgy. Over the past 20 years, he has studied welding and structure-property relationships in HSLA steels, aircraft grade aluminum alloys, metal-matrix and polymer-matrix composites.